CHAPTER 7

STABILITY AND FAILURE OF SUDDENLY LOADED LAMINATED COMPOSITE STIFFENED CYLINDRICAL PANEL

7.1 Introduction

In the previous chapter, the stability and failure of a laminated composite cylindrical panel with a centrally placed cutout were investigated. In this chapter, the stability and failure of a laminated composite stiffened cylindrical panel subjected to in-plane pulse load are investigated. The influence of parameters such as loading duration, loading function, aspect ratio of the stiffener and the stacking sequence on the stability and failure of laminated composite cylindrical panels is also investigated. This chapter is divided into the following sections:

- Convergence and Validation Studies
    - Convergence and Validation Studies of the Static Buckling Load of a Stiffened Plate
    - Validation of Static Buckling Load of a Cylindrical Panel
    - Validation of Natural Frequency of a Stiffened Plate
- Dynamic Buckling Studies
    - Effect of Loading Duration
    - Failure of Stiffened Cylindrical Panel
    - Effect of Loading Function
    - Effect of Curvature
    - Effect of the Aspect Ratio of the Stiffener
    - Effect of Ply Orientation

- Deformation of the Stiffened Cylindrical Panel

7.2 Convergence and Validation Studies

In this section, the results of convergence and validation studies are presented. For this, stiffened plate and stiffened cylindrical panels are considered and their static buckling loads are calculated.

7.2.1 Convergence and validation studies of the static buckling load of a stiffened plate

The convergence and validation studies of a stiffened plate are presented in this section. A square planed, simply supported stiffened plate is considered with geometric properties, b/a=1, b/h=100, b_s/h=2, d_s/b_s=2 and material properties E =2.11×10^{11}N/m^2 and υ=0.3. The width of the stiffener is denoted by 'b_s', 'd_s' is the depth of the stiffener and 'h' is the depth of the skin. Two stiffener orientations are considered for this case, one along the direction of loading (Fig. 7.1(a)) and one in the perpendicular direction (Fig. 7.2(a)).

The pre-buckling boundary conditions for the plate with stiffener along the direction of loading are shown in Fig. 7.1(b) and the buckling boundary conditions are shown in Fig. 7.1(c). Furthermore, the pre-buckling boundary conditions for the plate with a stiffener in the perpendicular direction of loading is shown in Fig. 7.2(b) and the buckling boundary conditions are shown in Fig. 7.2(b). The mesh size for the stiffener is 100×4 and for the skin is varied. This results in higher mesh density the junction of the skin and the stiffener.

Figure 7.3(a) shows the results of convergence study for the stiffened plate with stiffener along X-axis and loading along Y-axis i.e., stiffener along the direction of loading. Figure 7.3(b) shows the convergence study for laminated composite stiffened plate with stiffener along Y-axis and loading along Y-axis i.e., stiffener along the perpendicular direction of loading. In both Fig. 7.3(a) and Fig. 7.3(b), the total number of elements in the plate is shown. Table 7.1 shows the results of the present study and the finite element results of Patel *et al.* (2006). The non-dimensional static buckling load is calculated using Eqn. (7.1) where 'a' is the length of the loaded edge.

$$\overline{P_{cr}} = \frac{P_{cr}a^2}{D} \tag{7.1}$$

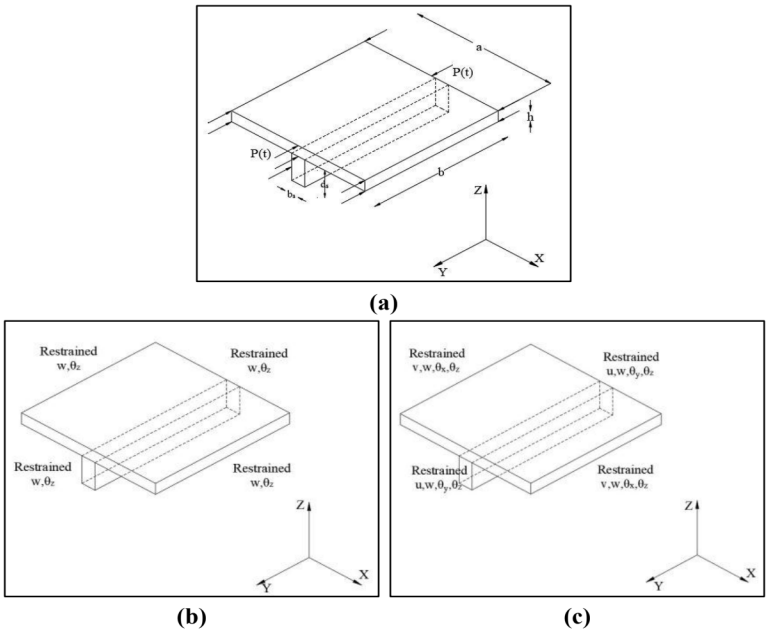

Fig. 7.1 Stiffened plate with a stiffener along the direction of loading **(a)** Geometry **(b)** Pre buckling boundary conditions **(c)** Buckling boundary conditions

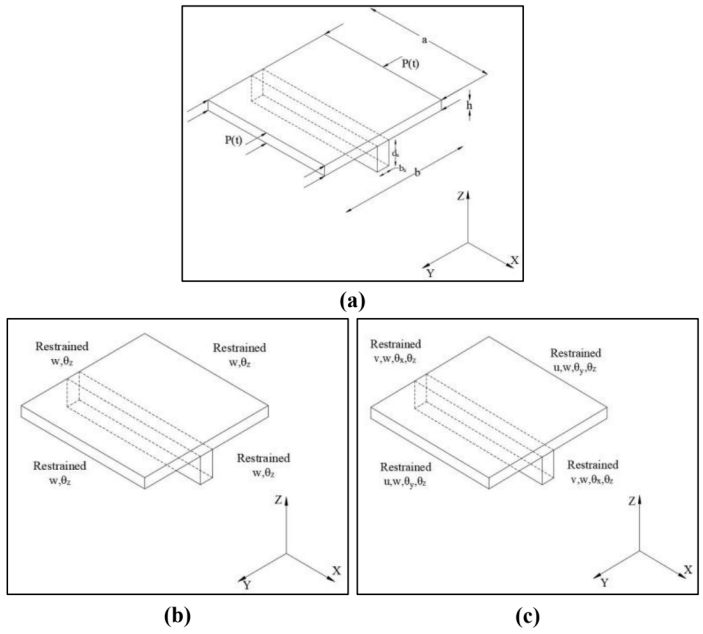

Fig. 7.2 Stiffened plate with a stiffener in the perpendicular direction of loading **(a)** Geometry **(b)** Pre buckling boundary conditions **(c)** Buckling boundary conditions

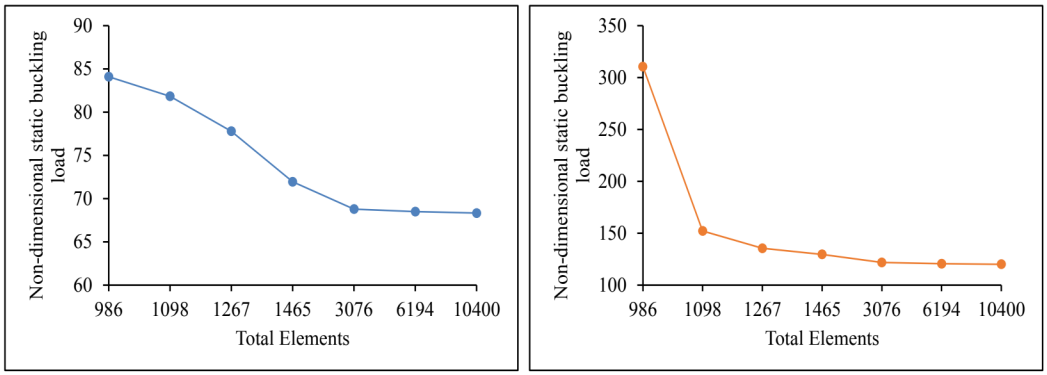

Fig. 7.3 Non-dimensional static buckling load for various mesh sizes for a stiffened plate **(a)** Stiffener in the perpendicular direction of loading **(b)** Stiffener along the direction of loading

Table 7.1 Non-dimensional static buckling load for a stiffened plate with b/a=1, b/h=100, b_s/h=2 and d_s/b_s=2

Analysis	**Non-dimensional static buckling load**	
	Stiffener perpendicular to the loading direction	**Stiffener along the loading direction**
Present	68.489	120.626
Patel e*t al.* (2006)	67.036	119.168
Error (%)	2.16	1.21

It is seen from Fig. 7.3(a) and Fig. 7.3(b) that the results converge at a total number of elements=6194. This corresponds to the mesh size of 100×4 in the stiffener and 50×50 in the skin. From Table 7.1, it is observed that the results of the present study match well with the finite element results of Patel *et al.* (2006).

7.2.2 Validation of static buckling load of a stiffened cylindrical panel

In this section, the results of the validation study of the static buckling load of a stiffened cylindrical panel are presented. The geometric properties of the cylindrical panel are R/a=2, b/a=1, b/h=100, b_s/h=2, d_s/b_s=2 and material properties E =2.11×10^{11}N/m^2 and υ=0.3. The geometry of the panel is shown in Fig. 7.4(a). The pre-buckling boundary conditions are shown in Fig. 7.4(b) and the buckling boundary conditions are shown in Fig. 7.4(c). The discretization of the panel is done in a similar way as done in the previous section, the mesh size for the stiffener is 100×4 and the mesh size for the skin is varied which results in higher mesh density

at the junction of the skin and the stiffener. The results of the present study are compared with the finite element results from Patel *et al.* (2006) in Table 7.2.

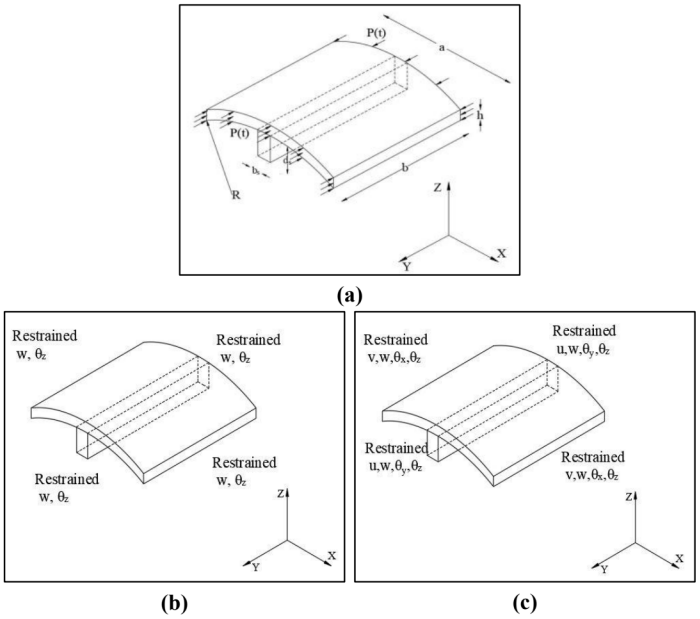

Fig. 7.4 Stiffened cylindrical panel for the validation study **(a)** Geometry **(b)** Pre-buckling boundary conditions **(c)** Buckling boundary conditions

Table 7.2 Non-dimensional static buckling load for the stiffened cylindrical panel with R/a=2, b/a=1, b/h=100, b_s/h=2 and d_s/b_s=2

Analysis	**Non-dimensional static buckling load**
Present	348.510
Patel *et al.* (2006)	347.952
Error (%)	0.16

From Table 7.2 it is observed that the result of the present study match with the finite element result from Patel *et al.* (2006). The total number of elements in the stiffened panel is 5489, which corresponds to 100×4 mesh divisions in the stiffener and 50×50 mesh divisions in the stiffener.

7.2.3 Validation of natural frequency of a stiffened plate

The results of the validation study of the natural frequency of a stiffened plate are presented in this section. The size of the plate is 203mm×203mm×1.37mm. and the size of the stiffener is

6.35mm×12.7mm. The material properties are E=7020kg/mm^2, ρ=2.72×10^{-10} kg-s^2/mm^4 and v=0.3. The plate is clamped on all four edges. Table 7.3 shows the results of the present study compared with the experimental results of Olson and Hazel (1977) and finite element results of Olson and Hazel (1977), Mukherjee and Mukhopadhyay (1988), Bhimaraddi et al. (1989), Sivasubramonian et al. (1999) and Nayak and Bandyopadhyay (2002). The error percentage for the FEM results and the experimental results (Olson and Hazel, 1977) of each author is shown in brackets in the table.

Table 7.3 Natural frequency of a stiffened plate with all edges clamped

Mode No.	Olsen and Hazell (1977)		Mukherjee and Mukhopadhyay (1988)	Bhimaraddi *et al.* (1989)	Sivasubramonian *et al.* (1999)	Nayak and Bandyopadhyay (2002)	Present
	Test	FEM	FEM	FEM	FEM	FEM	FEM
1	689	718.1	711.8	700.4	729.6	725.2	737.41
		(4.22)	(3.31)	(1.65)	(5.89)	(5.25)	(7.03)
2	725	751.4	768.2	737	748	745.3	768.36
		(3.64)	(5.96)	(1.66)	(3.17)	(2.80)	(5.98)
3	961	997.4	1016.5	966.6	1009.1	987.6	1017.6
		(3.79)	(5.78)	(0.58)	(5.01)	(2.77)	(5.89)
4	986	1007.1	1031.9	978.6	1016.6	994.4	1028.6
		(2.14)	(4.66)	(0.75)	(3.10)	(0.85)	(4.32)
5	1376	1419.8	1465.2	1380.1	1321.8	1401.9	1449.1
		(3.18)	(6.48)	(0.30)	(3.94)	(1.88)	(5.31)

From the table 7.3 it is observed that the FEM results of each author has less than 10% error compared to the experimental results of Olson and Hazel (1977). In each case, the authors have considered a different modelling technique. Olson and Hazel (1977) considered a triangular element with 9 degrees of freedom at each node and modeled the stiffener using refined beam bending and torsion elements. However, the authors reported that all the inertia terms were not considered. Mukherjee and Mukhopadhyay (1988) considered an eight noded isoparametric element with five degrees of freedom at each node and reported that good correlation exists amongst the results. Bhimaraddi *et al.* (1989) considered a quadrilateral shell element with 64 degrees of freedom with the incorporation of effects of rotary inertia and shear deformations. The authors attributed the better results to this. Sivasubramonian *et al.* (1999) considered a four noded shell element with seven degrees of freedom at each node and attributed the stiff shell to the assumption of zero shell rotary inertia and the linear transformation of shell displacement into those of the stiffener. Nayak and Bandyopadhyay (2002) presented the results with eight and nine noded shell elements with five degrees of freedom at each node. In Table 7.3, the results are presented with eight noded element. The authors reported that the error in the results

is negligible. In the present investigation, the a four noded shell element in conjunction with a three noded shell element with six degrees of freedom at each node are considered to model the stiffened plate. Further, the stiffener is modeled as a shell. Due to this reason, the error of the present results maybe on the higher side. However, the results from the present study are within 7.5% of the experimental results of Olson and Hazel (1977).

From the convergence and validation studies, it is seen that the result of the current study for static buckling and natural frequency match well with the results from the literature. In the succeeding sections, the simply supported boundary conditions used in the validation study are considered. The panel is discretized in a similar way as done in the validation study, i.e., the four edges of the skin of the panel are divided into 50 divisions and the stiffener is divided into 100 divisions along its length.

7.3 Dynamic Buckling Studies

The stability and failure of a laminated composite stiffened cylindrical panel subjected to in-plane pulse load are investigated in this section. The influence of duration of loading, stiffener aspect ratio, loading function and stacking sequence of skin and stiffener on the dynamic buckling behaviour of the cylindrical panel are also studied. The geometry of the panel is shown in Fig. 3.10(a) and the boundary conditions are shown in Fig. 3.10(b). The material properties are presented in Table 3.2. The procedure for calculating the dynamic buckling load and the first ply failure load is the same as presented in chapter 4 (section 4.3).

With the addition of a stiffener to a cylindrical panel, the static buckling of the panel changes. In the succeeding sections, the dynamic buckling load of the panel is compared with its corresponding static buckling load. The static buckling load and the first natural period of the stiffened cylindrical panel considered in the investigation are presented in Table 7.4. The geometric properties of the panel are: b/a=1, b/h=100 with a=0.1m with various radius of curvatures and aspect ratio of the stiffener.

Table 7.4 Static buckling load and first natural period of the stiffened cylindrical panel having b/a=1, b/h=100, d_s/b_s=2 with b=0.1m with various radius of curvatures and stacking schemes.

R/a	Stacking Scheme	d_s/b_s	Static Buckling Load (N/m)	First Natural Period (s)
20	(0°/90°/90°/0°)	1	22171	8.71×10^{-4}

(Table 7.4 Continued)

10	(0°/90°/90°/0°)	1	25256	1.72×10^{-3}
5	(0°/90°/90°/0°)	1	38449	1.37×10^{-3}
20	(45°/-45°/-45°/45°)	1	32540	1.67×10^{-3}
10	(45°/-45°/-45°/45°)	1	38750	1.35×10^{-3}
5	(45°/-45°/-45°/45°)	1	53102	8.71×10^{-4}
10	(0°/90°/90°/0°)	2	70194	5.97×10^{-4}
10	(0°/90°/90°/0°)	4	70589	5.91×10^{-4}
10	(0°/90°/90°/0°)	8	39797	1.30×10^{-3}
10	(0°/90°/90°/0°)	10	33170	1.54×10^{-3}
20	(0°/90°/90°/0°)	4	63857	6.39×10^{-4}
5	(0°/90°/90°/0°)	4	69197	6.17×10^{-4}
20	(45°/-45°/-45°/45°)	4	95602	9.15×10^{-4}
10	(45°/-45°/-45°/45°)	4	97210	8.67×10^{-4}
5	(45°/-45°/-45°/45°)	4	107197	7.18×10^{-4}
20	(0°/90°/90°/0°)	8	27830	1.65×10^{-3}
5	(0°/90°/90°/0°)	8	74829	5.91×10^{-4}
20	(45°/-45°/-45°/45°)	8	110050	6.80×10^{-4}
10	(45°/-45°/-45°/45°)	8	110879	6.78×10^{-4}
5	(45°/-45°/-45°/45°)	8	116882	6.67×10^{-4}
20	(0°/90°/90°/0°)	0	15238	2.08×10^{-3}
10	(0°/90°/90°/0°)	0	18212	1.9×10^{-3}
5	(0°/90°/90°/0°)	0	30848	1.41×10^{-3}
20	(45°/-45°/-45°/45°)	0	29975	1.66×10^{-3}
10	(45°/-45°/-45°/45°)	0	30949	1.32×10^{-3}
5	(45°/-45°/-45°/45°)	0	45934	8.41×10^{-4}

7.3.1 Effect of loading duration

In this section, the effect of loading duration on the stability and first ply failure of a stiffened cylindrical panel subjected to in-plane pulse load is presented. The panel with R/a=10, b/a=1, b/h=100, b_s/h=2 and d_s/b_s=1 is considered. Pulse load in the form of rectangular loading

function (Fig. 3.5(a)) is considered. Two stacking sequences are considered (0°/90°/90°/0°) and (45°/-45°/-45°/45°). The loading durations considered are ¼ T_n, ½ T_n, T_n, 2 T_n and 4T_n. Figure 7.5(a) shows the plot of non-dimensional load vs non-dimensional displacement for panel with R/a=10, d_s/b_s=1 and stacking sequence (0°/90°/90°/0°) for various durations of loading when subjected to rectangular pulse load. Figure 7.5(b) shows the plot of non-dimensional load vs non-dimensional displacement for panel with R/a=10, d_s/b_s=1 and stacking sequence (45°/-45°/-45°/45°) for various durations of loading when subjected to rectangular pulse load.

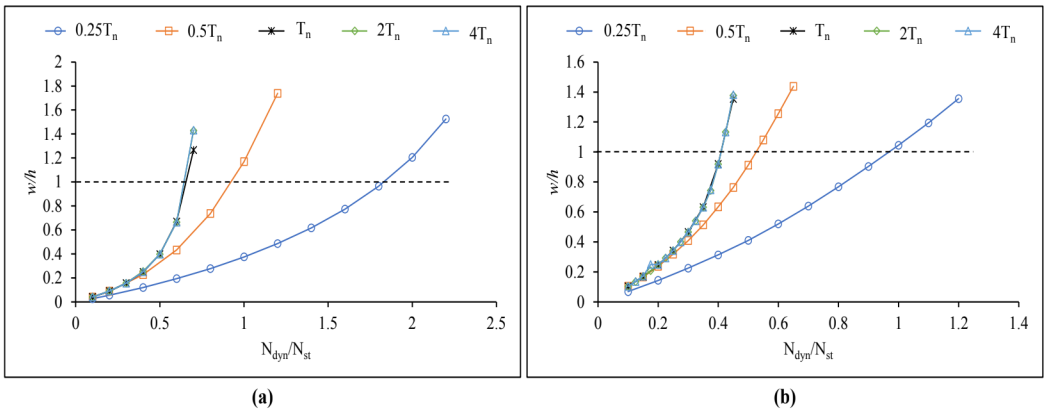

Fig. 7.5 Non-dimensional Load vs Non-dimensional Displacement for panel with R/a=10, d_s/b_s=1 and subjected to rectangular pulse load for various durations of loading **(a)** Stacking sequence (0°/90°/90°/0°) **(b)** Stacking sequence (45°/-45°/-45°/45°)

In Fig. 7.5 the static buckling load and the first natural period of the panel with stacking sequence (0°/90°/90°/0°) is different from the panel with stacking sequence is (45°/-45°/-45°/45°). In Fig. 7.5(a) the dynamic buckling load of the panel subjected till its first natural period (T_n) is 35% lower than its static buckling load. In Fig. 7.5(b) the dynamic buckling load of the panel subjected till its first natural period is 58% lower than its static buckling load. It is evident from Fig. 7.5(a) and Fig. 7.5(b) that when the duration of loading is very short, the dynamic buckling load of the stiffened cylindrical panel is high and when the duration of loading is increased, the dynamic buckling load for the stiffened panel decreases. No appreciable variation in response is observed when the loading duration is more than the first natural period of the cylindrical panel. The non-linear dynamic buckling load is lower than the static buckling load for all cases of loading durations considered for the stiffened panel when

the stacking sequence is (45°/-45°/-45°/45°). For the rest of the study, the duration of loading is taken as the first natural period of the respective panel.

7.3.2 Failure of stiffened cylindrical panel

The first ply failure of laminated composite stiffened cylindrical panel is studied in this section. The first ply failure load is calculated in order to check the precedence of dynamic buckling load and first ply failure load. The panel with R/a=10, b/a=1, b/h=100, b_s/h=2 and d_s/b_s=1 is considered. The panel is subjected to rectangular pulse load. The stacking sequence is (0°/90°/90°/0°).

Figure 7.6(a) shows the plot of non-dimensional load vs non-dimensional displacement for panel with R/a=10, d_s/b_s=1 and stacking sequence (0°/90°/90°/0°). Figure 7.6(b) shows the plot of N_{dyn}/N_{st} vs Failure Index for panel with R/a=10, d_s/b_s=1 and stacking sequence (0°/90°/90°/0°) for various failure theories. Figure 7.7(a) shows the deformed shape of the panel for maximum transverse displacement at N_{dyn}/N_{st} =0.7. Figure 7.7(b) shows the deformed shape of the panel for maximum failure index with respect to Tsai-Wu failure criterion at N_{dyn}/N_{st} =0.7. Figure 7.7(c) shows the deformed shape of the panel for maximum transverse displacement at N_{dyn}/N_{st} =1. Figure 7.7(d) shows the deformed shape of the panel for maximum failure index with respect to Tsai-Wu failure criterion at N_{dyn}/N_{st} =1. In Fig. 7.7(a) - Fig. 7.7(d), the panel is subjected to rectangular pulse load.

For the case of Figure 7.6(b), at N_{dyn}/N_{st}=1, the failure index is maximum at node 3996 which is at the junction of the skin and the stiffener. The failure index with respect to Tsai-Wu criterion at layer 1 is 1.1238, at layer 2 is 0.3406 at layer 3 is 0.3108 and at layer 4 is 0.6127. The numbering of the layers starts from the bottom to top in the increasing Z direction.

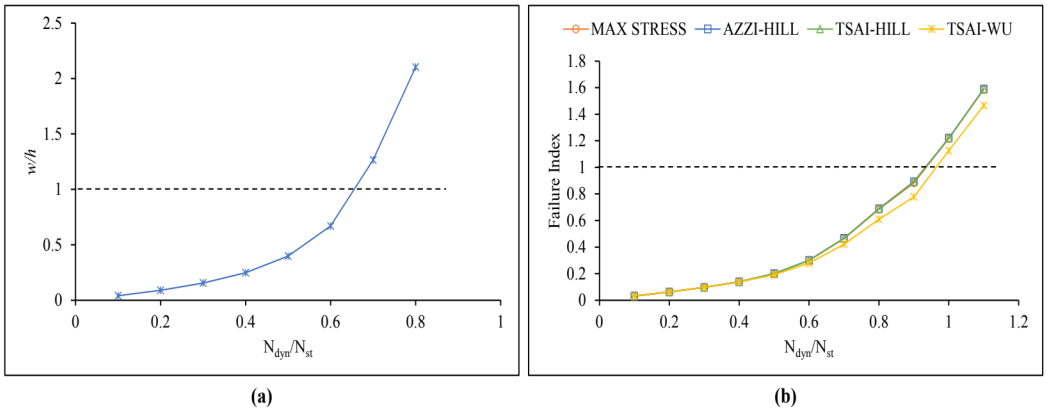

Fig. 7.6 Plot for a panel with R/a=10, d_s/b_s=1 and stacking sequence (0°/90°/90°/0°) subjected to rectangular pulse load **(a)** Non-dimensional Load vs non-dimensional Displacement **(b)** Non-dimensional Load vs Failure Index

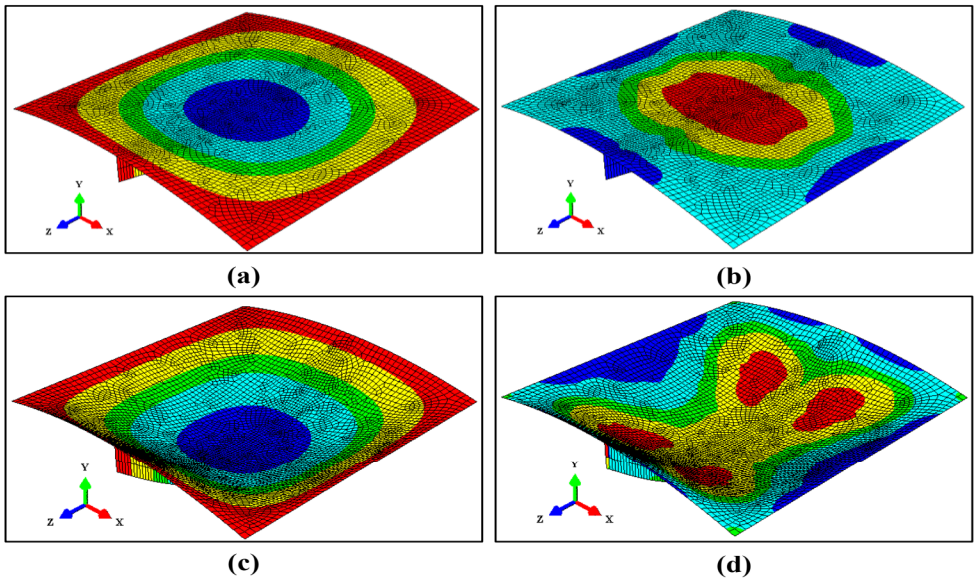

Fig. 7.7 Deformed shape of the stiffened cylindrical panel with R/a=10, d_s/b_s=1 and stacking sequence (0°/90°/90°/0°) subjected to rectangular pulse load. Scale Factor = 3 **(a)** For maximum transverse displacement at N_{dyn}/N_{st} =0.7 **(b)** For maximum failure index (Tsai-Wu criterion) at N_{dyn}/N_{st} =0.7. **(c)** For maximum transverse displacement at N_{dyn}/N_{st} =1 **(d)** For maximum failure index (Tsai-Wu criterion) at N_{dyn}/N_{st} =1

From Fig. 7.6(b) it is seen that the failure index for the panel is close to the static buckling load (4% lower) and the failure indices are very close to each other. The deformed shape of the

panel shows that the dynamic buckling occurs at the centre of the panel and the first ply failure occurs at the junction of the skin and the stiffener. The enlarged area is shown in Fig. 7.17. In Fig. 7.6(b) although higher failure indices are shown, progressive failure is not investigated. In Fig. 7.7(a) and Fig. 7.7(c), the region in blue colour at the centre of the panel is the area of maximum deformation. In Fig. 7.7(b) and Fig. 7.7(d), the region in red colour shows the area of the maximum failure index. The scale factor is provided in Y-direction only. The undeformed shape with equal scale in all directions is shown in Fig. 7.16 for reference.

7.3.3 Effect of loading function

The effect of rectangular and sinusoidal pulse loading function on the stability and first ply failure of a stiffened cylindrical panel is studied in this section. The cylindrical panel with b/a=1, b/h=100, b_s/h=2 and d_s/b_s=1 is considered. The stacking sequence is (0°/90°/90°/0°). The rectangular pulse loading function and sinusoidal pulse loading functions are shown in Fig. 3.5(a) and Fig. 3.5(b) respectively. The radius of curvature considered is R/a=20, and R/a=10. The stiffened panel is subjected to in-plane pulse load till its first natural period.

Figure 7.8(a) and Fig. 7.8(b) show the plot of non-dimensional load vs non-dimensional displacement for the panel with stacking sequence (0°/90°/90°/0°) subjected to both pulse loading functions for the stiffened panel with R/a=20 and R/a=10 respectively. Figure 7.8(c) and Fig. 7.8(d) show the plot of non-dimensional load vs failure index with respect to Tsai-Wu failure criterion for the panel with stacking sequence (0°/90°/90°/0°) subjected to both loading functions for the stiffened panel with R/a=20 and R/a=10 respectively.

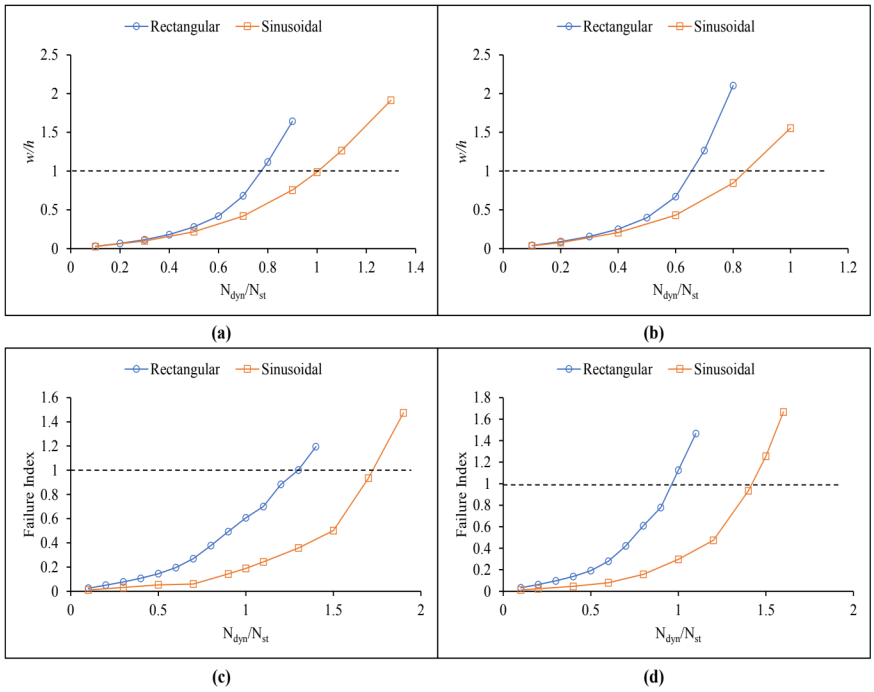

Fig. 7.8 Plot for a stiffened cylindrical panel with d_s/b_s=1 and stacking sequence (0°/90°/90°/0°) for both pulse loading functions. **(a)** Non-dimensional Load vs non-dimensional Displacement for panel with R/a=20 **(b)** Non-dimensional Load vs non-dimensional Displacement for panel with R/a=10 **(c)** Non-dimensional Load vs Failure Index (Tsai-Wu criterion) for panel with R/a=20 **(d)** Non-dimensional Load vs Failure Index (Tsai-Wu criterion) for panel with R/a=10

The value of Nst in Fig. 7.8(a) and 7.8(b) are different. With the change in curvature of the panel, the static buckling load of the panel changes and the dynamic buckling load of the panels are compared with their respective static buckling loads.

In Fig. 7.8 (a) it is observed that for the panel with R/a=20 and d_s/b_s=1, the dynamic buckling load of the panel when subjected to rectangular in-plane pulse load is 23% lower than its static buckling load and when the panel is subjected to sinusoidal in-plane pulse load, its dynamic buckling load is equal to its static buckling load. In Fig. 7.8 (b) it is observed that for the panel with R/a=10 and d_s/b_s=1, the dynamic buckling load of the panel when subjected to rectangular in-plane pulse load is 34% lower than its static buckling load and when the panel is subjected to sinusoidal in-plane pulse load, its dynamic buckling load is 16% lower than its static buckling load.

In Fig. 7.8 (c) it is observed that for the panel with R/a=20 and d_s/b_s=1, the first ply failure load of the panel when subjected to rectangular in-plane pulse load is 30% higher than its static buckling load and when the panel is subjected to sinusoidal in-plane pulse load, its first ply failure load is 72% higher than static buckling load. In Fig. 7.8 (d) it is observed that for the panel with R/a=10 and d_s/b_s=1, the first ply failure load of the panel when subjected to rectangular in-plane pulse load is 4% lower than its static buckling load and when the panel is subjected to sinusoidal in-plane pulse load, its first ply failure load is 42% higher than its static buckling load.

These results signify that the dynamic buckling load of the stiffened panel is lower when the panel is subjected to rectangular pulse loading compared to the panel subjected to sinusoidal pulse load. This is because higher energy is imparted into the system when a rectangular loading function is used. The same phenomenon is observed in a composite plate, the cylindrical panel with and without a cutout. It is also observed that in both cases of curvatures, the dynamic buckling load is lower than the first ply failure load and the corresponding static buckling load. The strength and stiffness of the stiffened panel is lower when subjected to rectangular in-plane pulse load than when subjected to in-plane sinusoidal pulse load.

7.3.4 Effect of curvature

The effect of the curvature of the stiffened panel on the stability and first ply failure of the panel subjected to in-plane pulse load is studied in this section. Panel with b/a=1, b/h=100, b_s/h=2 and d_s/b_s=1 is considered. The stacking sequence is (0°/90°/90°/0°) and (45°/-45°/-45°/45°). Three curvatures are considered. R/a=20, R/a=10 and R/a=5. The panel is subjected to rectangular in-plane pulse load till its first natural period and the responses are observed after the removal of the load.

Figure 7.9(a) and Fig. 7.9(b) show the plot of non-dimensional load vs non-dimensional displacement for the panel with d_s/b_s=1 for various radius of curvatures having stacking sequence (0°/90°/90°/0°) and (45°/-45°/-45°/45°) respectively. Figure 7.9(c) and Fig. 7.9(d) show the plot of non-dimensional load vs failure index with respect to Tsai-Wu failure criterion for panel with d_s/b_s=1 for various radius of curvatures having stacking sequence (0°/90°/90°/0°) and (45°/-45°/-45°/45°) respectively.

In Fig. 7.9, the static buckling load (N_{st}) of the stiffened panel changes with the change in the curvature of the panel and also with the change in the ply orientation of the panel. In each case, the dynamic buckling load of the panel is compared with its static buckling load. In Fig. 7.9(a) it is observed that the stiffened panel with balanced and symmetric cross-ply laminates, having d_s/b_s=1 and R/a=5, 10 and 20, corresponding the dynamic buckling load of the panels are 46%, 34% and 23% lower than their respective static buckling loads. In Fig. 7.9(b) it is observed that the stiffened panel with balanced and symmetric angle-ply laminates, having d_s/b_s=1 and R/a=5, 10 and 20, corresponding the dynamic buckling load of the panels are 55%, 59% and 45% lower than their respective static buckling loads.

In Fig. 7.9(c) it is observed that the stiffened panel with balanced and symmetric cross-ply laminates, having d_s/b_s=1 and R/a=5 and 10 corresponding the first ply failure load of the panels are 31% and 4% lower than their respective static buckling loads. the first ply failure load of the panel with R/a=20 is 30% higher than its static buckling load. In Fig. 7.9(d) it is observed that the stiffened panel with balanced and symmetric angle-ply laminates, having d_s/b_s=1 and R/a=5, 10 and 20, corresponding the first ply failure load of the panels are 53%, 58% and 43% lower than their respective static buckling loads.

The dynamic buckling load of the panels are lower than their corresponding first ply failure loads. these results show that the stiffness and the strength of the panels change with the change in curvature of the panels.

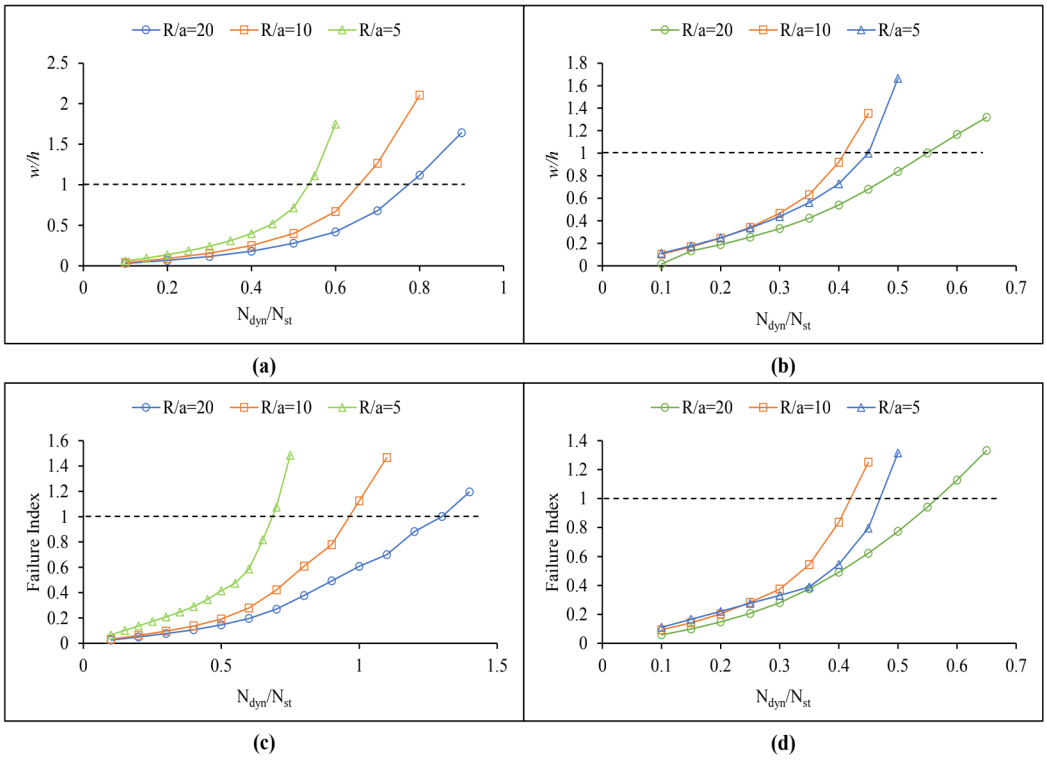

Fig. 7.9 Plot for the stiffened panel with d_s/b_s=1 and subjected to rectangular pulse load for various radius of curvatures **(a)** Non-dimensional Load vs non-dimensional Displacement for panel with stacking sequence (0°/90°/90°/0°) **(b)** Non-dimensional Load vs non-dimensional Displacement for panel with stacking sequence (45°/-45°/-45°/45°) **(c)** Non-dimensional Load vs Failure Index (Tsai-Wu criterion) for panel with stacking sequence (0°/90°/90°/0°) **(d)** Non-dimensional Load vs Failure Index (Tsai-Wu criterion) for panel with stacking sequence(45°/-45°/-45°/45°)

7.3.5 Effect of the aspect ratio of the stiffener

In this section, the effect of the aspect ratio of the stiffener on the stability and first ply failure of a stiffened cylindrical panel subjected to in-plane pulse load is studied. The panel with R/a=10, b/a=1, b/h=100 and b_s/h=2 is considered. The stacking sequence is (0°/90°/90°/0°). The panel is subjected to rectangular pulse load till its first natural period. The thickness of the stiffener is kept the same and the depth of the stiffener is varied. The various aspect ratios considered are d_s/b_s = 0,1,2,4,8 and 10. Panel with d_s/b_s = 0 signifies unstiffened cylindrical panel.

Figure 7.10 shows the plot of non-dimensional load vs non-dimensional displacement for the stiffened panel with R/a=10, b_s/h=2 and stacking sequence (0°/90°/90°/0°) subjected to rectangular pulse load for various stiffener aspect ratios. Figure 7.11 shows the plot of non-dimensional load vs failure index with respect to Tsai-Wu failure criterion for the stiffened panel with R/a=10, b_s/h=2 and stacking sequence (0°/90°/90°/0°) subjected to rectangular pulse load for various stiffener aspect ratios.

With the change in the aspect ratio of the stiffener, the static buckling load of the panel changes. When a stiffener is attached to the panel with R/a =10 in order to make it more stiff, the static buckling load of the now stiffened panel changes. As the depth of the stiffener increases, the dynamic buckling load and the first ply failure load of the stiffened panel compared to the unstiffened panel will keep increasing. In the present investigation, the dynamic buckling load of the stiffened panel is compared with its corresponding static buckling load. This is done to check at what stiffener depth the dynamic buckling load and the first ply failure load of the stiffened panel will be higher than its static buckling load.

It is observed from Fig. 7.10 that the dynamic buckling load of the panel with R/a=10 having balanced and symmetric laminates changes significantly with the change in the depth of the stiffener. The dynamic buckling loads of the panel with d_s/b_s=1 and d_s/b_s=2 are 34% and 36% lower than their respective static buckling loads. And, the dynamic buckling loads of the panel with d_s/b_s=4, d_s/b_s=8 and d_s/b_s=10 are 26%, 24% and 27% higher than their respective static buckling loads.

It is observed from Fig. 7.11 that the first ply failure load of the panel with R/a=10 having balanced and symmetric laminates changes also changes in a similar way with the change in the depth of the stiffener. The first ply failure loads of the panel with d_s/b_s=1 and d_s/b_s=2 are 4% and 25% lower than their respective static buckling loads. And, the first ply failure loads of the panel with d_s/b_s=4, d_s/b_s=8 and d_s/b_s=10 are 2%, 1% and 11% higher than their respective static buckling loads.

These results are further discussed in the next section where the effect of stacking sequence on the dynamic buckling behaviour and the failure of the stiffened cylindrical panel with various aspect ratios of the stiffener is investigated.

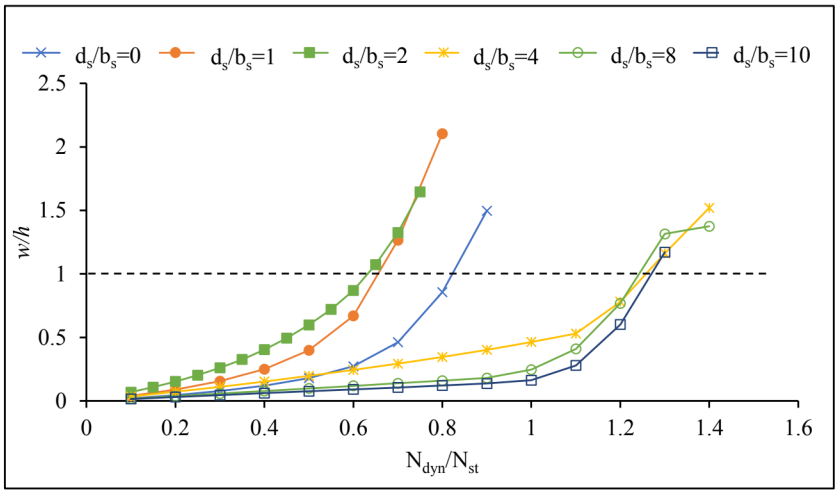

Fig. 7.10 Non-dimensional Load vs non-dimensional Displacement for the stiffened panel with *R/a* =10, b_s/h=2 and stacking sequence (0°/90°/90°/0°) subjected to rectangular pulse load for various aspect ratios of stiffeners

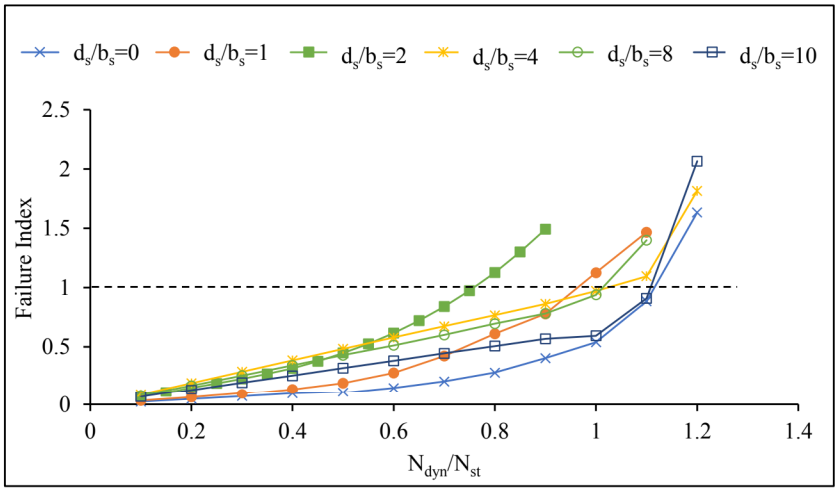

Fig. 7.11 Non-dimensional Load vs Failure Index (Tsai-Wu criterion) for the stiffened panel with *R/a*=10, b_s/h=2, and stacking sequence (0°/90°/90°/0°) subjected to rectangular pulse load for various aspect ratios of stiffeners.

7.3.6 Effect of stacking sequence

In this section, the effect of stacking sequence on the stability and failure of a laminated composite stiffened cylindrical panel subjected to in-plane pulse load is studied. The panel with *b/a*=1, *b/h*=100 and b_s/h=2 is considered. The panel is subjected to rectangular pulse load till

its first natural period. The radius of curvatures considered are R/a=20, R/a=10 and R/a=5. The stacking sequences in the stiffened panel are (0°/90°/90°/0°) and (45°/-45°/-45°/45°). Aspect ratios of the stiffeners are d_s/b_s =0,1,4 and 8. Panel with d_s/b_s =0 refers to the unstiffened cylindrical panel.

Figure 7.12(a) shows the plot of non-dimensional load vs non-dimensional displacement for panel with R/a=20 and stacking sequence (0°/90°/90°/0°) for various stiffener aspect ratios. Figure 7.12(b) shows the plot of non-dimensional load vs non-dimensional displacement for panel with R/a=10 and stacking sequence (0°/90°/90°/0°) for various stiffener aspect ratios. Figure 7.12(c) shows the plot of non-dimensional load vs non-dimensional displacement for panel with R/a=5 and stacking sequence (0°/90°/90°/0°) for various stiffener aspect ratios. Figure 7.12(d) shows the plot of non-dimensional load vs failure index with respect to Tsai-Wu criterion for panel with R/a=20 and stacking sequence (0°/90°/90°/0°) for various stiffener aspect ratios. Figure 7.12(e) shows the plot of non-dimensional load vs failure index with respect to Tsai-Wu criterion for panel with R/a=10 and stacking sequence (0°/90°/90°/0°) for various stiffener aspect ratios. Figure 7.12(f) shows the plot of non-dimensional load vs failure index with respect to Tsai-Wu criterion for panel with R/a=5 and stacking sequence (0°/90°/90°/0°) for various stiffener aspect ratios.

Figure 7.13(a) shows the plot of non-dimensional load vs non-dimensional displacement for panel with R/a=20 and stacking sequence (45°/-45°/-45°/45°) for various stiffener aspect ratios. Figure 7.13(b) shows the plot of non-dimensional load vs non-dimensional displacement for panel with R/a=10 and stacking sequence (45°/-45°/-45°/45°) for various stiffener aspect ratios. Figure 7.13(c) shows the plot of non-dimensional load vs non-dimensional displacement for panel with R/a=5 and stacking sequence (45°/-45°/-45°/45°) for various stiffener aspect ratios. Figure 7.13(d) shows the plot of non-dimensional load vs failure index with respect to Tsai-Wu criterion for panel with R/a=20 and stacking sequence (45°/-45°/-45°/45°) for various stiffener aspect ratios. Figure 7.13(e) shows the plot of non-dimensional load vs failure index with respect to Tsai-Wu criterion for panel with R/a=10 and stacking sequence (45°/-45°/-45°/45°) for various stiffener aspect ratios. Figure 7.13(f) shows the plot of non-dimensional load vs failure index with respect to Tsai-Wu criterion for panel with R/a=5 and stacking sequence (45°/-45°/-45°/45°) for various stiffener aspect ratios.

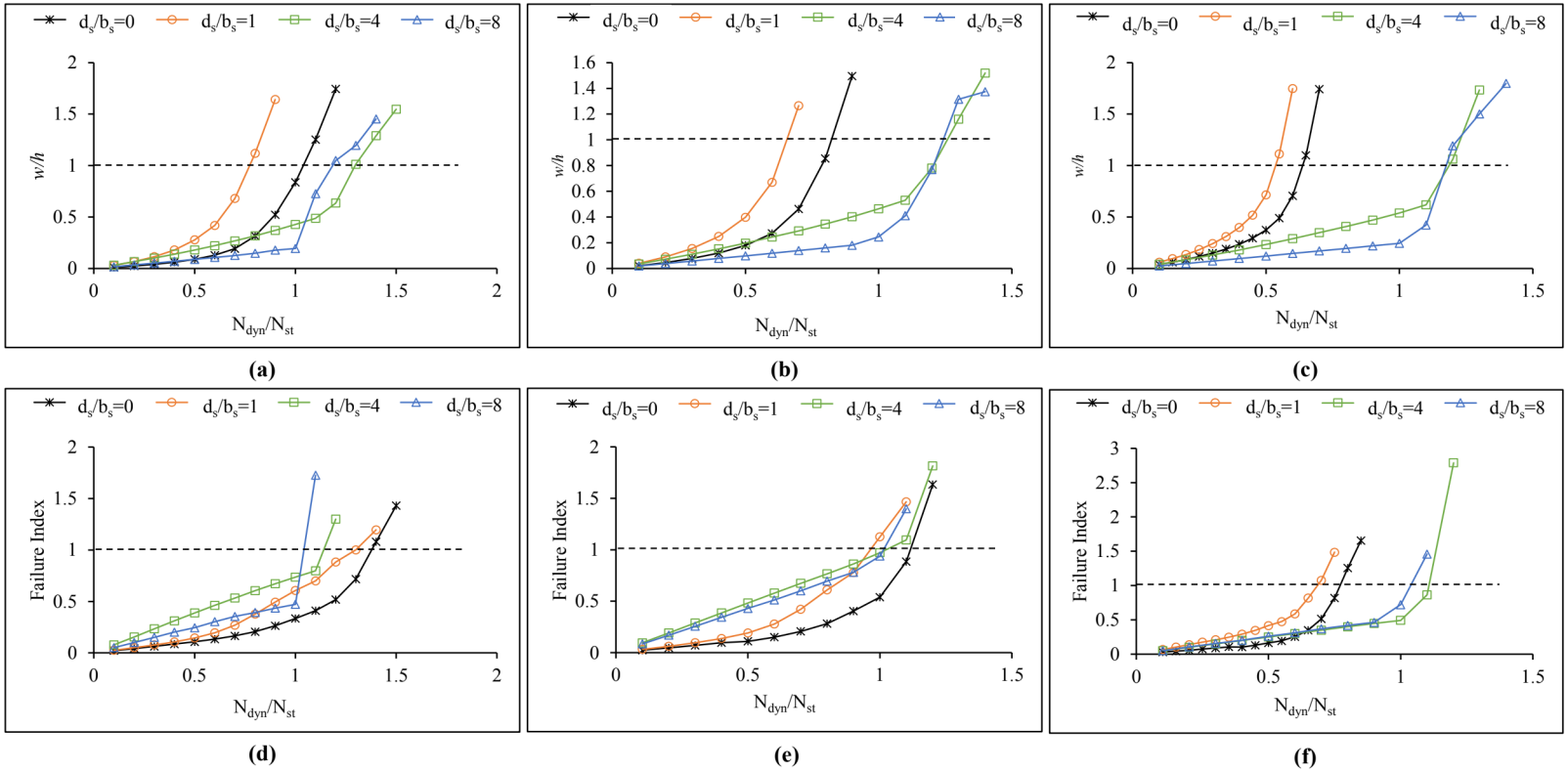

Fig. 7.12 Plot for the stiffened panel with stacking sequence (0°/90°/90°/0°) for various stiffener aspect ratios. **(a)** Non-dimensional Load vs non-dimensional Displacement for panel with *R/a*=20 **(b)** Non-dimensional Load vs non-dimensional Displacement for panel with *R/a*=10 **(c)** Non-dimensional Load vs non-dimensional Displacement for panel with *R/a*=5 **(d)** Non-dimensional Load vs Failure Index (Tsai-Wu criterion) for panel with *R/a*=20 **(e)** Non-dimensional Load vs Failure Index (Tsai-Wu criterion) for panel with *R/a*=10 **(f)** Non-dimensional Load vs Failure Index (Tsai-Wu criterion) for panel with *R/a*=5

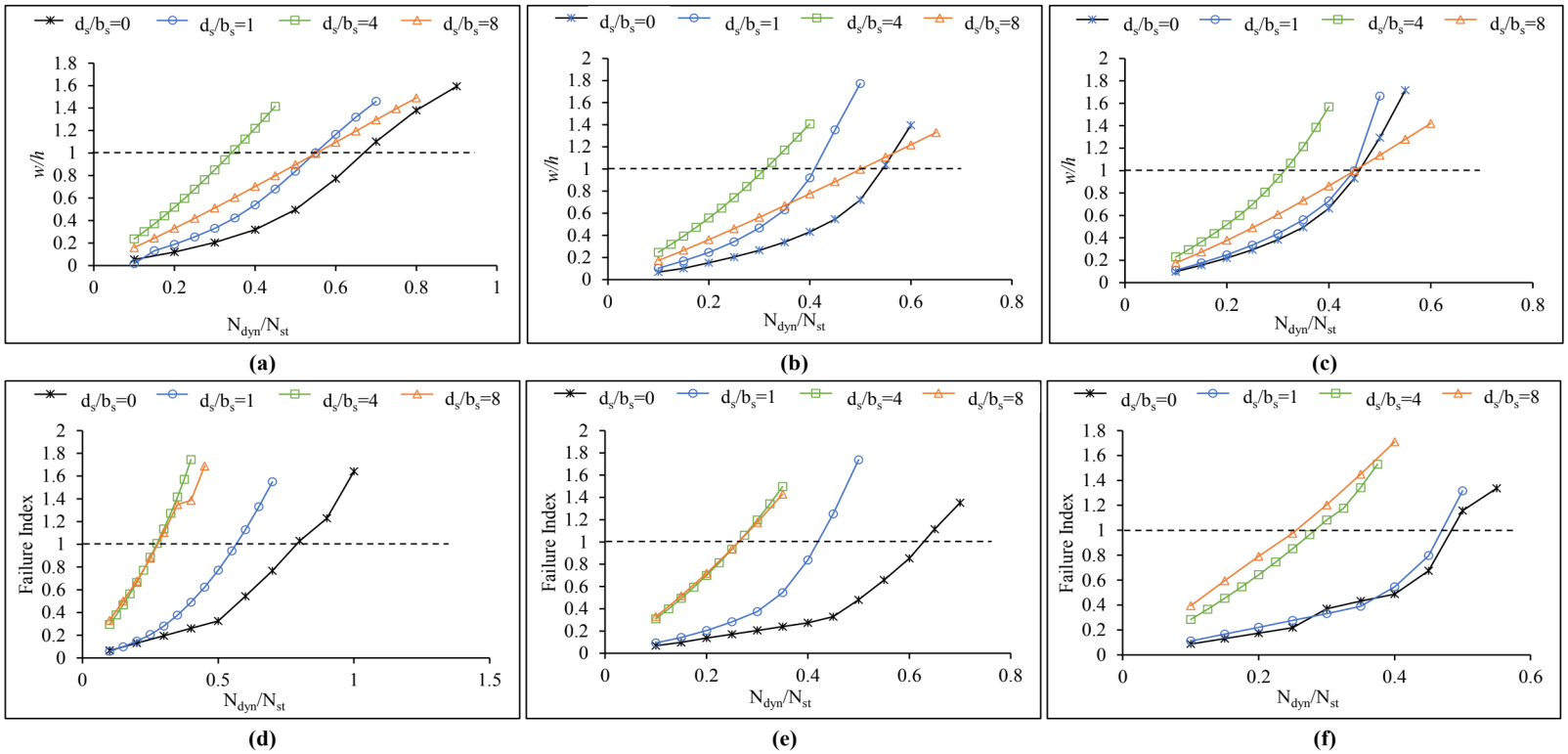

Fig. 7.13 Plot for the stiffened panel with stacking sequence (45°/-45°/-45°/45°) for various stiffener aspect ratios. **(a)** Non-dimensional Load vs non-dimensional Displacement for panel with *R/a*=20 **(b)** Non-dimensional Load vs non-dimensional Displacement for panel with *R/a*=10 **(c)** Non-dimensional Load vs non-dimensional Displacement for panel with *R/a*=5 **(d)** Non-dimensional Load vs Failure Index (Tsai-Wu criterion) for panel with *R/a*=20 **(e)** Non-dimensional Load vs Failure Index (Tsai-Wu criterion) for panel with *R/a*=10 **(f)** Non-dimensional Load vs Failure Index (Tsai-Wu criterion) for panel with *R/a*=5

It is observed in Fig. 7.12, in all the cases of curvatures considered, the panel with balanced and symmetric cross-ply laminates, having d_s/b_s=1 has its dynamic buckling load lower than its static buckling load. The dynamic buckling load of the panel with d_s/b_s=1 and R/a=5, 10 and 20 is 46%, 34% and 23% lower than the corresponding static buckling load. Also, for this stiffener aspect ratio, the first ply failure loads of panel with R/a=5 and 10 are 32%, 4% lower than its corresponding static buckling load. For the panel with R/a=20, the panel with d_s/b_s=1 has 30% higher first ply failure load than its static buckling load.

The dynamic buckling loads of the panel with balanced and symmetric cross-ply laminates having d_s/b_s=4 and different radius of curvatures, R/a=5, 10 and 20 are 19%, 26% and 30% higher than their corresponding static buckling loads. Similarly, the dynamic buckling loads of the panel with balanced and symmetric cross-ply laminates having d_s/b_s=8 and different radius of curvatures, R/a=5, 10 and 20 are 17%, 24% and 18% higher than their corresponding static buckling loads.

The first ply failure loads of the panel with balanced and symmetric cross-ply laminates having d_s/b_s=4 and different radius of curvatures, R/a=5, 10 and 20 are 11%, 2% and 14% higher than their corresponding static buckling loads. Similarly, the first ply failure loads of the panel with balanced and symmetric cross-ply laminates having d_s/b_s=8 and different radius of curvatures, R/a=5, 10 and 20 are 4%, 1% and 4% higher than their corresponding static buckling loads.

In the case of the stiffened cylindrical panel with angel-ply laminates, the dynamic buckling load and the first ply failure load of the panel for the radius of curvatures considered and the stiffener depth consider are lower than the corresponding static buckling loads. The dynamic buckling loads of the panel with angle-ply laminates and R/a=5 with d_s/b_s=1,4 and 8 are 55%, 69% and 55% lower than the corresponding static buckling loads. The dynamic buckling loads of the panel with angle-ply laminates and R/a=10 with d_s/b_s=1,4 and 8 are 59%, 69% and 50% lower than the corresponding static buckling loads. The dynamic buckling loads of the panel with angle-ply laminates and R/a=20 with d_s/b_s=1,4 and 8 are 45%, 66% and 45% lower than the corresponding static buckling loads.

The first ply failure loads of the panel with angle-ply laminates and R/a=5 with d_s/b_s=1,4 and 8 are 53%, 72% and 74% lower than the corresponding static buckling loads. The first ply failure loads of the panel with angle-ply laminates and R/a=10 with d_s/b_s=1,4 and 8 are 58%,

74% and 74% lower than the corresponding static buckling loads. The first ply failure loads of the panel with angle-ply laminates and R/a=20 with d_s/b_s=1,4 and 8 are 43%, 73% and 73% lower than the corresponding static buckling loads.

These results signify that the stiffened cylindrical panels with angle-ply laminates have lower stiffness and strength than the panels with cross-ply laminates when subjected to rectangular in-plane pulse loads. With the addition of stiffener, although the mass of the panel is increased, the combination of mass and stiffness of the stiffened panel is harmful to the cylindrical panel. Hence, in the case of angle-ply laminates, stiffeners with aspect ratio (d_s/b_s) till 8 may not be suitable in the dynamic environment. These results also signify that when the orientation of plies is along the direction of loading, the non-linear dynamic buckling load is higher than the static buckling load and first ply failure load if the aspect ratio of the stiffener is at least 4.

Figure 7.14(a) shows the deformed shape of the panel for maximum transverse displacement with R/a=10, d_s/b_s=1 and (45°/-45°/-45°/45°) at N_{dyn}/N_{st} =0.4. Figure 7.14(b) shows the deformed shape of the panel for maximum transverse displacement with R/a=10, d_s/b_s=4 and (45°/-45°/-45°/45°) at N_{dyn}/N_{st} =0.325. Figure 7.14(c) shows the deformed shape of the panel for maximum transverse displacement with R/a=10, d_s/b_s=8 and stacking sequence (45°/-45°/-45°/45°) at N_{dyn}/N_{st} =0.5. Figure 7.15(a) shows the deformed shape of the panel for maximum failure index with respect to Tsai-Wu failure criterion with R/a=10, d_s/b_s=1 and stacking sequence (45°/-45°/-45°/45°) at N_{dyn}/N_{st} =0.45. Figure 7.15(b) shows the deformed shape of the panel for maximum failure index with respect to Tsai-Wu failure criterion with R/a=10, d_s/b_s=4 and stacking sequence (45°/-45°/-45°/45°) at N_{dyn}/N_{st} =0.275. Figure 7.15(c) shows the deformed shape of the panel for maximum failure index with respect to Tsai-Wu failure criterion with R/a=10, d_s/b_s=8 and stacking sequence (45°/-45°/-45°/45°) at N_{dyn}/N_{st} =0.3.

The scale factor is provided in Y-direction only. The undeformed shapes are shown in Fig. 7.16-7.21 for reference. In Fig. 7.14 and Fig. 7.15, global buckling is observed when the aspect ratio of the panel is 1 and 4. The first ply failure occurs at the corners of the panel. This signifies that the stacking sequence is critical when panels are operating in a dynamic environment. In Fig. 7.14(a), 7.14(b) and 7.14(c), the region in blue colour represents the area with maximum displacement. In Fig. 7.15(a), 7.15(b) and 7.15(c), the region in red colour represents the area with maximum Failure Index.

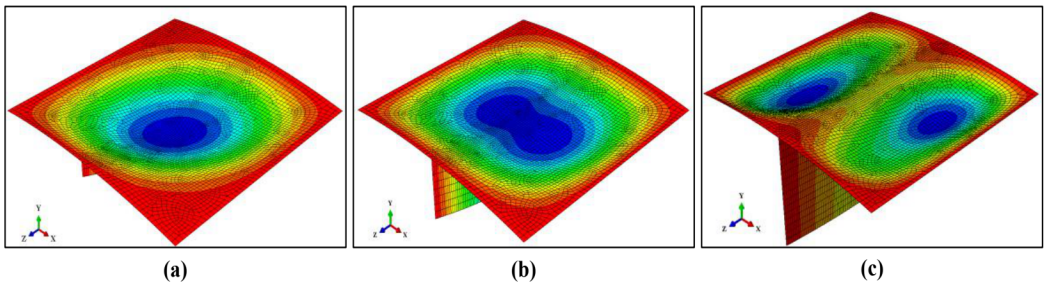

Fig. 7.14 Deformed shape of the stiffened panel for maximum transverse displacement having R/a=10 and stacking sequence (45°/-45°/-45°/45°) **(a)** Panel with d_s/b_s=1 at N_{dyn}/N_{st} =0.4 **(b)** Panel with d_s/b_s=4 at N_{dyn}/N_{st} =0.325 **(c)** Panel with d_s/b_s=8 at N_{dyn}/N_{st} =0.5

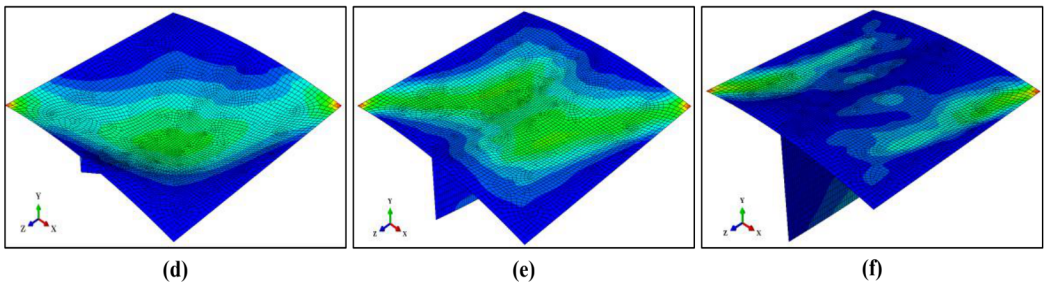

Fig. 7.15 Deformed shape of the stiffened panel for Tsai-Wu failure criterion having R/a=10 and stacking sequence (45°/-45°/-45°/45°) **(a)** Panel with d_s/b_s=1 at N_{dyn}/N_{st} =0.45 **(b)** Panel with d_s/b_s=4 at N_{dyn}/N_{st} =0.275 **(c)** Panel with d_s/b_s=8 at N_{dyn}/N_{st} =0.3

7.3.7 Deformation of stiffened cylindrical panel

In this section, the deformation of the stiffened panel is presented. Although the deformed shapes of the panels at dynamic buckling load and first ply failure load are presented in the previous sections, the evolution of the deformation is presented in this section. For this panel with b/a=1, b/h=100, R/a=10 and b_s/h=2 is considered. The stacking sequence is (0°/90°/90°/0°). The panel is subjected to rectangular pulse load. The aspect ratio of the stiffener considered is d_s/b_s=1,4 and 8.

In Fig. 7.16-Fig. 7.21, for the deformed shapes, different scale factors are given for the panels for better representation. Also, the scale factor is provided in Z-direction only. Due to this, the length of the stiffener seems to be unrealistic. For this reason, an undeformed shape with equal scale factor in all directions is also shown.

Figure 7.16, 7.18 and 7.20 show the plot of non-dimensional load vs non-dimensional displacement for the stiffened panel with R/a=10 and stacking sequence (0°/90°/90°/0°) subjected to rectangular pulse load for stiffener aspect ratio 1, 4 and 8 respectively along with deformed shapes of the stiffened panel at various magnitude of loads. Figure 7.17, 7.19 and 7.21 show the plot of non-dimensional load vs failure index with respect to Tsai- Wu failure criterion for panel with R/a=10 and stacking sequence (0°/90°/90°/0°) subjected to rectangular pulse load for stiffener aspect ratio 1, 4 and 8 respectively along with deformed shapes of the stiffened panel at various magnitude of loads.

In Fig. 7.16, the maximum deformation in the panel is observed at the centre of the stiffened panel which is shown in blue colour. In Fig. 7.17, the location of the maximum failure index changes with change in the magnitude of the applied dynamic in-panel pulse load which is shown in red colour. At the locations marked as '9' and '10', the maximum failure Index is observed at the junction of skin and the stiffener near the loaded edges, which are also shown. In Fig. 7.18 and 7.20, the maximum deformation in the stiffened panel is observed in the skin of the panel. Also, in Fig. 7.19 and 7.21, the location of the maximum failure index changes with the change in the magnitude of the applied dynamic pulse load. Due to the change in the deformed shape of the stiffened panel, i.e., from overall deformation of the panel (skin and the stiffener) to local deformation (only in the skin) at dynamic buckling load, the stiffened panel with d_s/b_s=4 and 8 show a sharp increase in displacement when subjected to a dynamic pulse load near the dynamic buckling load of the stiffened panel. Furthermore, for the same reason, a sharp increase in the maximum failure index is also observed in the stiffened panel with d_s/b_s=4 and 8.

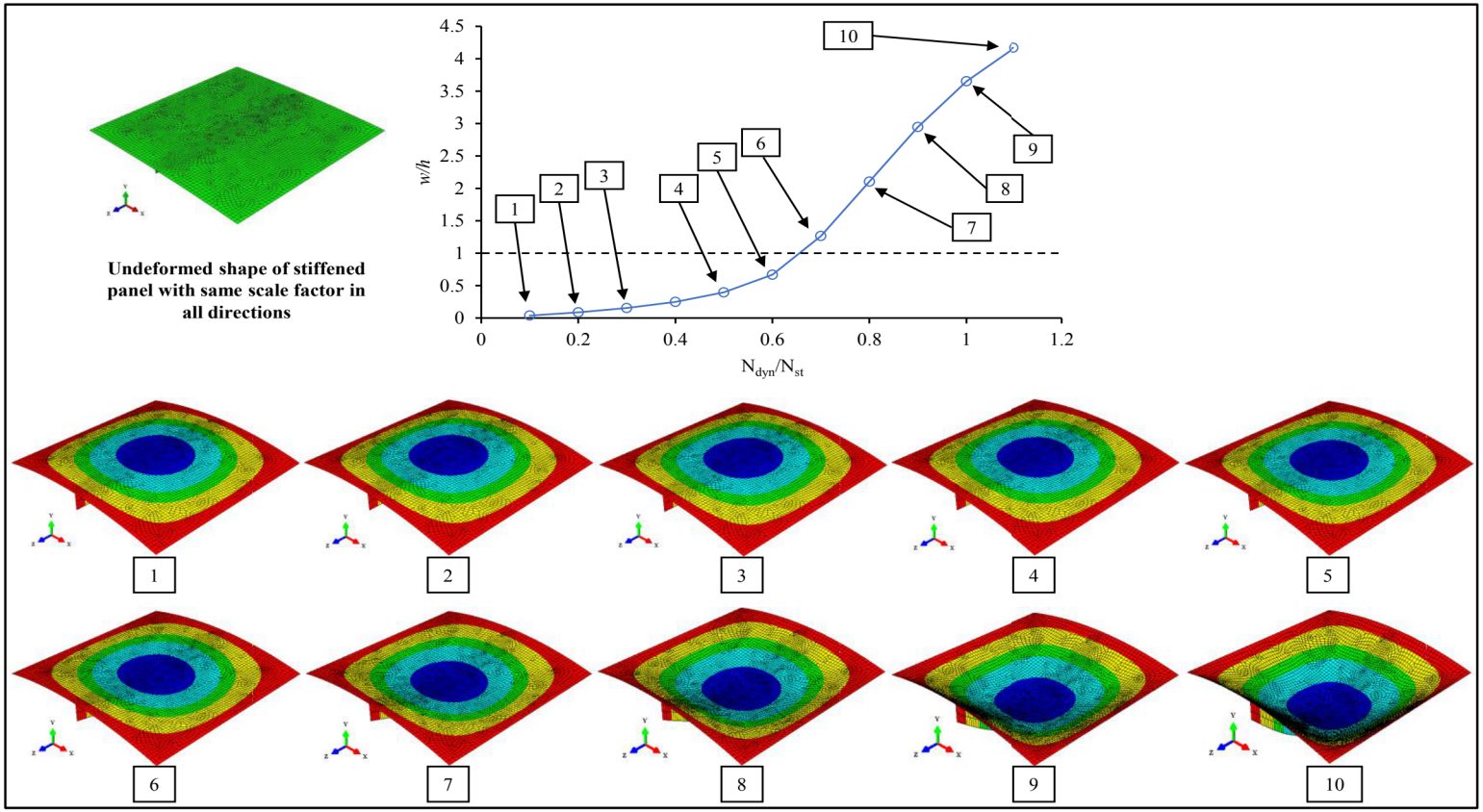

Fig. 7.16 Non-dimensional Load vs non-dimensional Displacement for the stiffened panel with R/a=10, d_s/b_s=1 and stacking sequence (0°/90°/90°/0°) subjected to rectangular pulse load along with deformed shape of the stiffened panel at various magnitude of loads. Scale Factor=5.

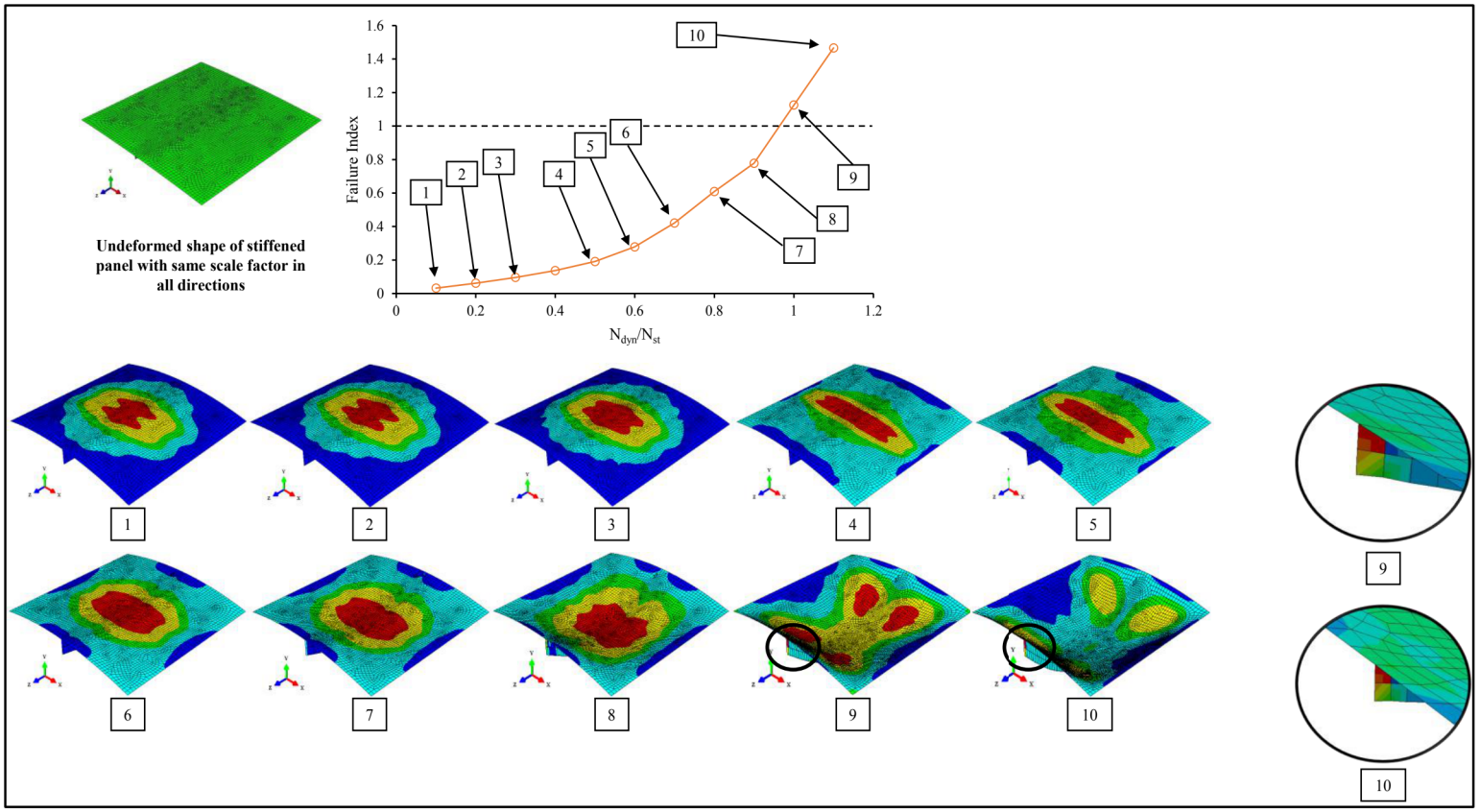

Fig. 7.17 Non-dimensional Load vs Failure Index (Tsai-Wu criterion) for the stiffened panel with R/a=10, d_s/b_s=1 and stacking sequence (0°/90°/90°/0°) subjected to rectangular pulse load along with deformed shape of the stiffened panel at various magnitude of loads. Scale Factor=5.

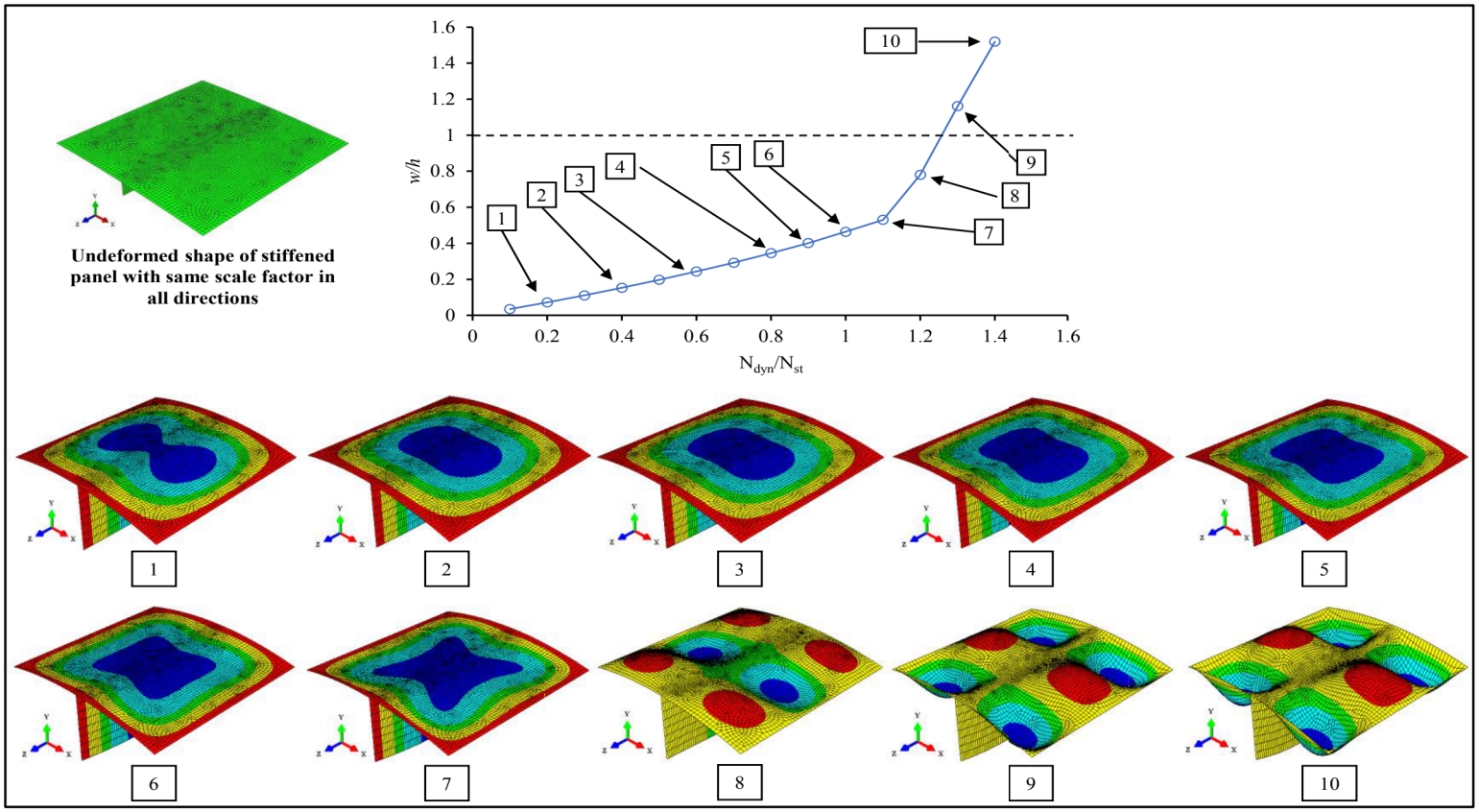

Fig. 7.18 Non-dimensional Load vs non-dimensional Displacement for the stiffened panel with R/a=10, d_s/b_s=4 and stacking sequence (0°/90°/90°/0°) subjected to rectangular pulse load along with deformed shape of the stiffened panel at various magnitude of loads. Scale Factor=5.

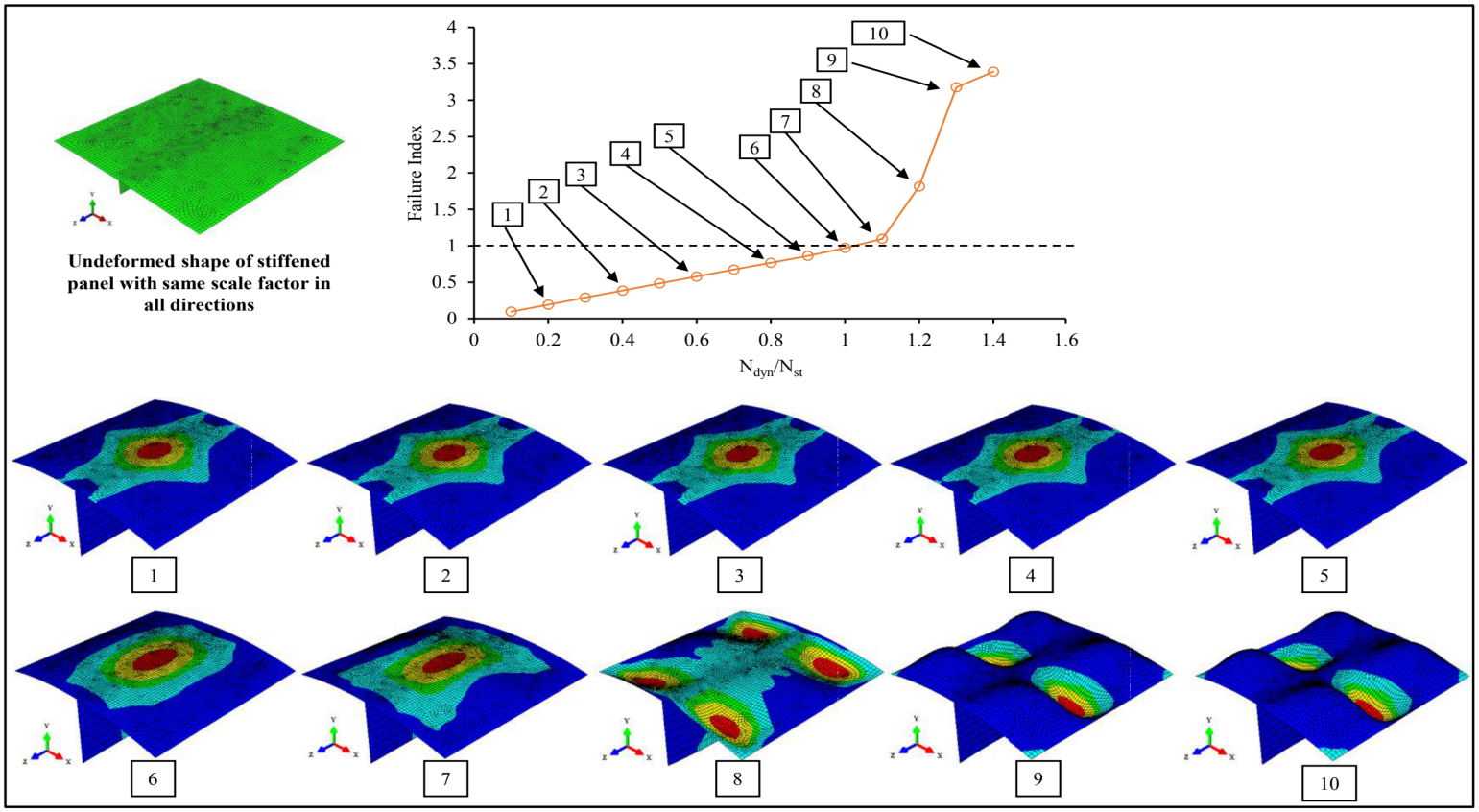

Fig. 7.19 Non-dimensional Load vs Failure Index (Tsai-Wu criterion) for the stiffened panel with R/a=10, d_s/b_s=4 and stacking sequence (0°/90°/90°/0°) subjected to rectangular pulse load along with deformed shape of the stiffened panel at various magnitude of loads. Scale Factor=5.

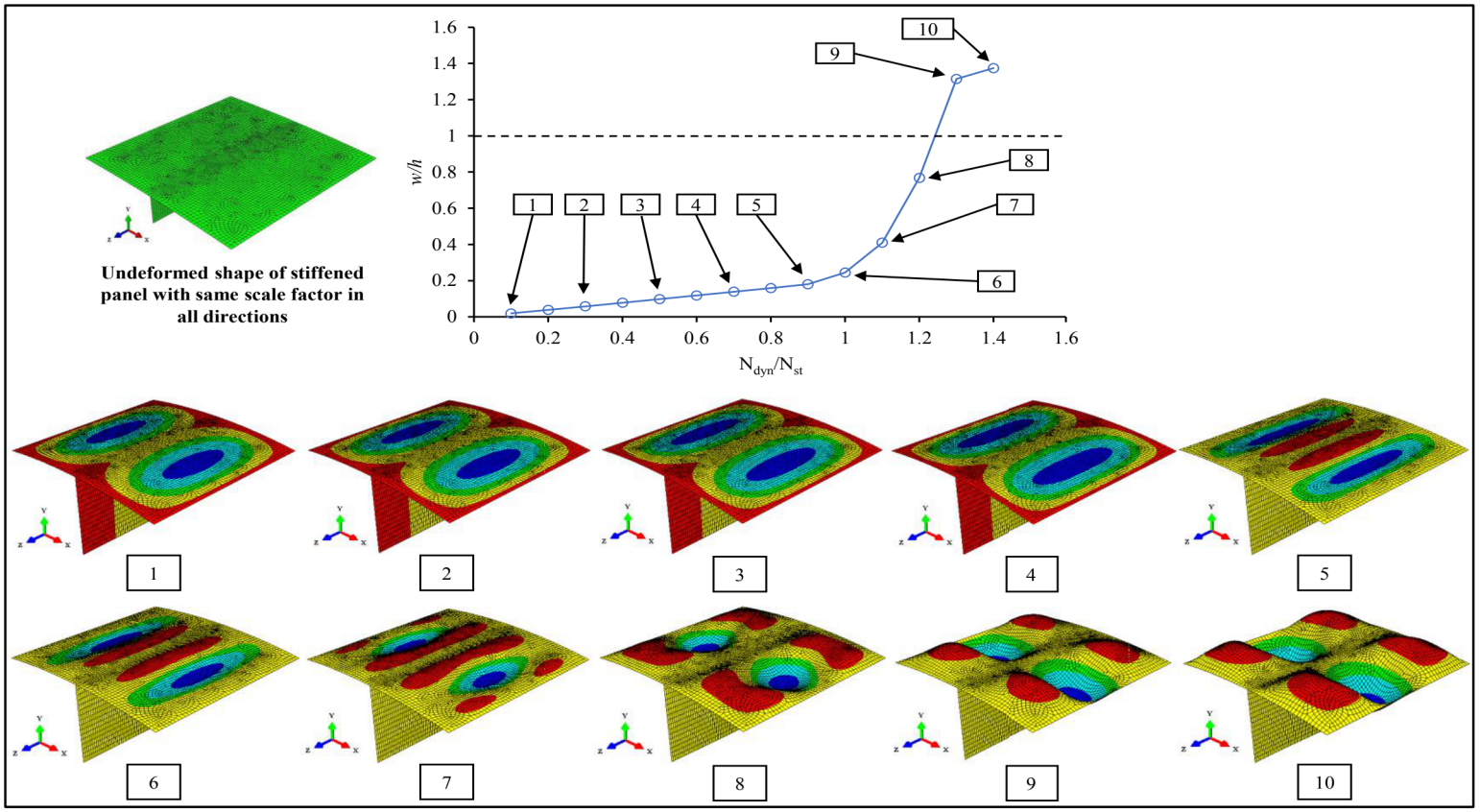

Fig. 7.20 Non-dimensional Load vs non-dimensional Displacement for the stiffened panel with R/a=10, d_s/b_s=8 and stacking sequence (0°/90°/90°/0°) subjected to rectangular pulse load along with deformed shape of the stiffened panel at various magnitude of loads. Scale Factor=3.5.

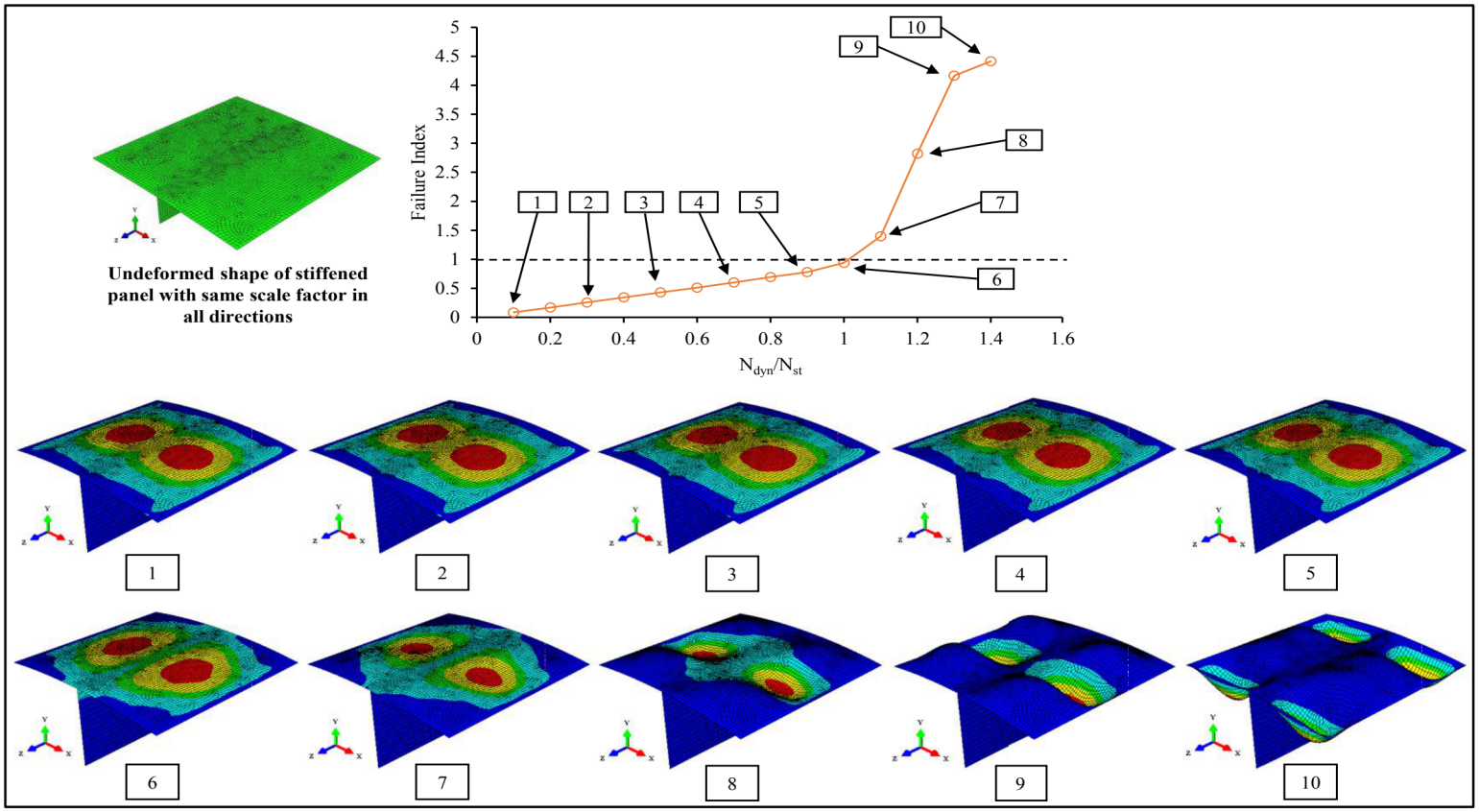

Fig. 7.21 Non-dimensional Load vs Failure Index (Tsai-Wu criterion) for the stiffened panel with R/a=10, d_s/b_s=8 and stacking sequence (0°/90°/90°/0°) subjected to rectangular pulse load along with deformed shape of the stiffened panel at various magnitude of loads. Scale Factor=3.5.

7.4 Summary

The stability and the first ply failure of a laminated composite stiffened panel subjected to in-plane pulse load are investigated in this chapter. The influence of various parameters such as loading duration, loading function, curvature, stacking sequence and the aspect ration of the stiffener on the stability and the first ply failure of the stiffened panel subjected to in-plane pulse load is studied. The conclusions of the study are presented in Chapter 8 (section 8.6).